Peer-reviewed version available at *Biomolecules* **2018**, *8*, 120; doi:10.3390/biom8040120

Review

Modeling membrane-protein interactions

Haleh Alimohamadi and Padmini Rangamani*

Department of Mechanical and Aerospace Engineering, University of California San Diego, CA 92093, USA

* Correspondence: prangamani@ucsd.edu; Tel.: +1-858-534-4734

Abstract: In order to alter and adjust the shape of the membrane, cells harness various mechanisms of curvature generation. Many of these curvature generation mechanisms rely on the interactions between peripheral membrane proteins, integral membrane proteins, and lipids in the bilayer membrane. One of the challenges in modeling these processes is identifying the suitable constitutive relationships that describe the membrane free energy that includes protein distribution and curvature generation capability. Here, we review some of the commonly used continuum elastic membrane models that have been developed for this purpose and discuss their applications. Finally, we address some fundamental challenges that future theoretical methods need to overcome in order to push the boundaries of current model applications.

Keywords: Plasma membrane; Spontaneous curvature; Helfrich energy; Area difference elastic model; Protein crowding; Deviatoric curvature

1. Introduction

The ability of cellular membranes to bend and adapt their configurations is critical for a variety of cellular functions including membrane trafficking processes [1,2], fission [3,4], fusion [5,6], differentiation [7], cell motility [8,9], and signal transduction [10–12]. In order to dynamically reshape the membrane, cells rely on a variety of molecular mechanisms from forces exerted by the cytoskeleton [13–15] and membrane-protein interactions [16–19]. Each mechanism induces unique surface stresses on the membrane and these surface stresses can be mapped onto the shape to understand the mechanical aspects of membrane deformation [20–23].

The interplay between cellular membrane and membrane proteins is one of the major sources of curvature production in live cells. Membrane protein interactions result not only from those proteins that are integral to the membrane but also from those proteins, such as scaffolding molecules or GTPases that can attach and detach from the membrane surface locally in response to signaling events. [17,18,24–27]. Many different mechanisms have been proposed for how proteins can generate curvature of the membrane; for the purposes of theoretical modeling and capturing the key physical principles, the broadly accepted mechanisms can be grouped into two main categories; (*i*) the hydrophobic insertion mechanism, and (*ii*) coat proteins with hydrophilic domains [18,28,29]. In the hydrophobic insertion mechanism, membrane bending occurs due to the change in the relative area of the two membrane leaflets, which happens due to partially embedded amphipathic

helices of the protein domains [30,31]. In contrast, when proteins are thought to coat the membrane, there is no insertion into lipid bilayer and proteins simply oligomerize along the membrane surface [32,33]. In this case, it has been suggested that the steric pressure generated due to protein crowding and scaffolding drive the membrane deformation [34–36].

There are various methods to visualize membrane curvatures *in situ* or in reconstituted systems such as X-ray crystallography [48,49], nuclear magnetic resonance spectroscopy (NMR) [50,51], fluorescence microscopy [52,53], and electron

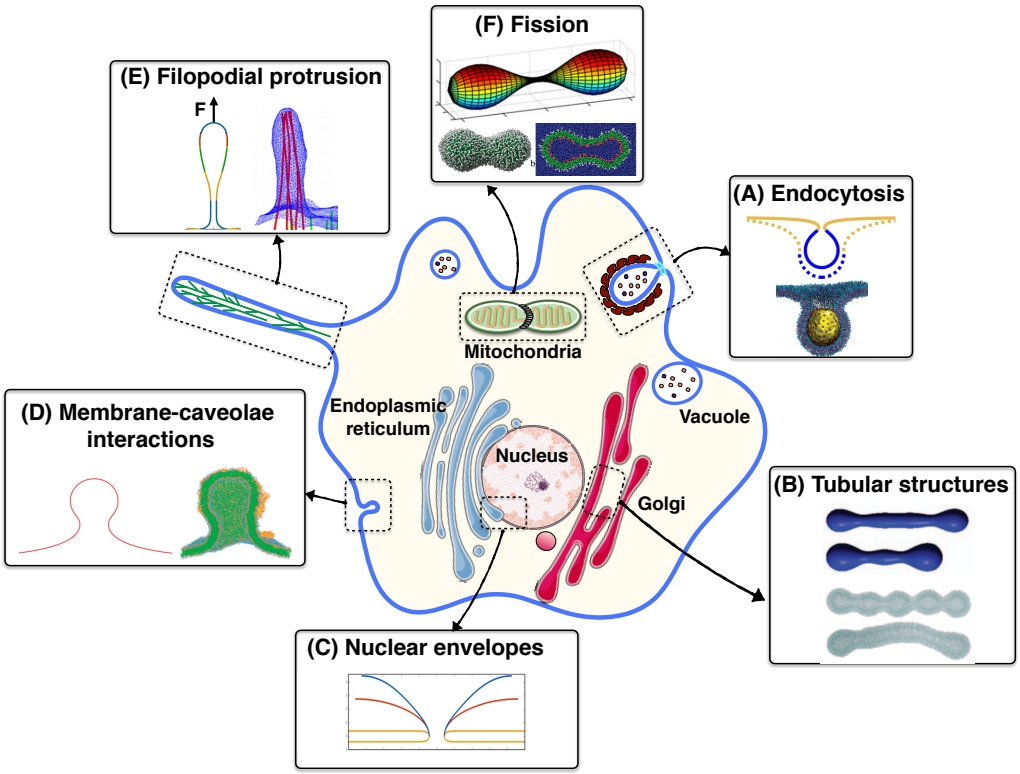

Figure 1. Membrane curvature generation in cells and associated modeling approaches. (A) Membrane budding in endocytosis, continuum approach [37] (top), molecular dynamics approach [38] (bottom). (B) Formation and stabilization of tubular membrane structures in the Golgi, continuum approach [39] (top), molecular dynamic approach [40] (bottom). (C) Change in the topology of nuclear envelopes, continuum approach [41], (D) Membrane invagination in caveolae, continuum approach [42] (left), molecular dynamic approach [43] (right). (E) Actin force driven filopodia protrusion, continuum approach [44] (left), molecular dynamics approach [45] (right). (F) Mitochondrial fission, continuum approach [46] (top), molecular dynamics approach [47] (bottom).

In this review article, we mainly focus on continuum models for incorporating the effects of membrane proteins on lipid bilayers and cell membranes. In section 2, we briefly introduce the basic components of biological membranes and highlight their structure and functions. Next, in section 3 we present the two different computational approaches for modeling membrane-protein interaction – molecular dynamics versus continuum models. In section 4, we provide an overview of some of the popular continuum models for describing the constitutive relationships of the plasma membranes in contact with proteins. We conclude the review with a discussion on the challenges and possible future directions of the theoretical methods in section 5.

2. Membrane-protein interactions

2.1. Biological membranes

Biological membranes (BMs) are fundamental architectures that form the outer boundary of living cells or compartments inside the cell. BMs act as semi-impermeable barriers that separate the cell contents from the extracellular environment while they also allow the vital materials to pass into or out of the cell [66,67]. The main component of all biological membranes is a lipid bilayer. The lipid bilayer thickness is about 5-10 nm and is made of three primary lipids: phospholipids, cholesterol, and glycolipid molecules (see Fig. 2) [67–69]. Proteins are the second major component of cell membranes in which the weight ratio of the lipids to membrane proteins can vary from 20% to 70%, depending on the cell type [67,70,71]. Proteins in cell membranes are classified into two categories; integral and peripheral proteins [72,73] (see Fig. 2). The third major component of BMs is carbohydrate molecules, which are found on the extracellular side of cell membranes. [74,75]. Carbohydrates are usually short and branched chains consisting of plain sugars, amino sugars, and acidic sugars. We briefly survey the different classes of membrane proteins, their functions, and their structures in cell membranes in what follows.

2.2. Integral proteins

Integral proteins are embedded permanently in the membrane by hydrophobic, electrostatic, and other non-covalent interactions [76,77]. Therefore, removing integral proteins from lipid bilayer is only possible by the use of detergents or nonpolar solvents that break down the strong membrane-protein interactions. The most common type of integral proteins are transmembrane proteins, which span across the lipid bilayer such that one end contacts the cell interior and the other end touches the exterior. When proteins cross the lipid bilayer, they usually adopt an α-helical configuration (Fig. 2) [73,78]. Single-pass membrane proteins cross the membrane only once, while the multiple-pass membrane proteins are crossing the membrane several times. Many of the integral membrane proteins function as ion channels or transporters, regulating the influx of ions/molecules between the extracellular and intracellular spaces. Cell surface receptors, linkers, enzymatic proteins, and proteins responsible for cell adhesion [66] are all classes of integral membrane proteins and hormone receptors, Band3, rhodopsin, histocompatibility antigens, glycophorin, and Na^+ and K^+ channels are some examples of integral proteins in a cell membrane. Recent studies have shown that activity of these proteins depends on the lipid composition and membrane-protein interactions more so than previously thought [79,80], highlight the role of lipids in the activity of these molecules fundamental for biological information transfer [81–83].

2.3. Peripheral proteins

Peripheral proteins temporarily bind to the surface of the membrane with weak interactions [76,84]. This means that unlike integral proteins, peripheral proteins can be easily separated from lipid bilayer by either altering the pH or the salt concentration of the cell culture medium [67]. A peripheral protein can have different structures, but there are

two key aspects that each structure should have. First, peripheral protein have a unique amino acid sequence which allows them to bind and congregate on the surface of the membrane [85,86]. Second, there is no hydrophobic region of amino acids in peripheral proteins structure, therefore they can attach to membrane surface without being locked onto it [85,86]. Classic examples of peripheral proteins include Cytochrome c, spectrin in erythrocytes, myelin basic protein, and acetylcholinesterase in electroplax membranes [87,88]. The primary role of peripheral proteins is to provide a point of attachment for other components to the cell membrane. For instance, both membrane cytoskeleton and components of extracellular matrix are linked to the cell membrane through peripheral proteins, thus they help the cell to maintain its shape while the membrane remains flexible to bend based on the cellular functions [89]. Besides the structural supports, peripheral proteins are involved in various other functions including cell communication, energy transduction, and molecule transfer across the membrane [89].

2.4. Glycoproteins

Glycoproteins are a class of proteins which have carbohydrate chains (in the form of oligosaccharides) covalently attach to the main protein body [90,91]. The presence of carbohydrate chains can dramatically alter the intrinsic properties of a glycoprotein such as the size, charge, solubility, structure, and accessibility [92]. Depending on how and where carbohydrate chains attach to the protein, the glycoproteins are classified into three categories; N-linked glycoproteins, O-linked glycoproteins, and non-enzymatic glycosylated glycoproteins [90,93]. In N-linked glycoproteins, the carbohydrate chains are attached to the the nitrogen atoms of the amino acid asparagine. In O-linked glycoproteins, the carbohydrate chains are linked to the hydroxyl side chain of amino acids serine or threonine. In the third group, unlike the two others, the non-enzymatic glycosylated glycoproteins are synthesized by chemical addition of carbohydrate chains to polypeptides [73,90]. In terms of functionality, glycoproteins are almost found in all living organisms and serve a number of important roles as structural molecules, immunologic molecules, transport molecules, receptors, enzymes, and hormones [90,94]. For instance, the glycoproteins on the membrane surface form bonds with the extracellular matrix, helping the cell stabilize

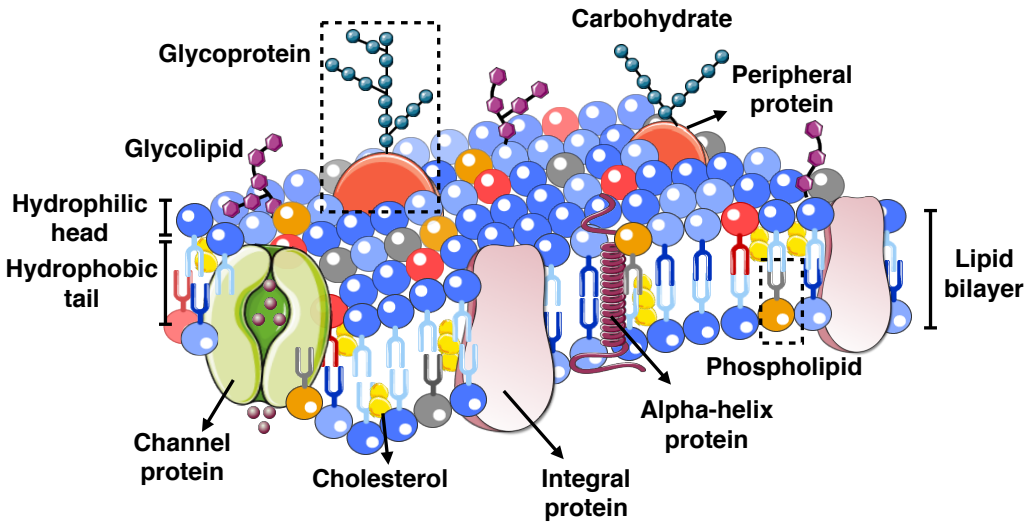

Figure 2. Schematic depiction of the composition of a cellular membrane. There are two layers of amphipathic lipid molecules that self-assemble to form the bilayaer. In each layer, the hydrophilic head groups form the outer surface and the hydrophobic tails face toward each other in the interior region. The distribution and organization of lipids and different proteins can vary from cell to cell. The cell membrane is decorated with many different molecules including peripheral proteins, integral proteins, and carbohydrate molecules.

its membrane structure. In addition to that, the glycoproteins receptors and antigens facilitate cell-cell recognition and interaction which are a key factor for immune system functionality [94].

3. Theoretical models of biological membranes

3.1. Mechanical viewpoint

Theoretical approaches are complementary techniques that have been developed in the last few decades to how cells regulate their function through geometry, mechanics, and signaling. [11,58,95–97]. In general, theoretical approaches can be classified into discrete and continuum models. In discrete models, the equations describe atoms' motion with in interaction with each other, through a set of bonded and non-bonded potentials, are solved by Molecular Dynamics (MD) or Coarse-Grained (CG) simulation techniques [98,99]. Tracing all atoms in a system makes this model suitable for exploring the nature of the biological process at the molecular level such as the biochemistry underlying the lipid-lipid or lipid-protein interactions, which are typically very difficult to detect experimentally. However, the high computational cost of MD or CG simulations limit the applications of discrete models just to phenomena at nanoscopic length and time scales [95,100,101].

On the other hand, there is a continuum approach that deals with the membrane as a continuous surface with average properties [95]. Indeed, the small length scale of the membrane constituents ($\sim$ 3-6 nm) compared to the length scales of biological phenomena ($\sim$ 100 nm-μm) allows us to define the complex membrane as a single continuum surface [95]. The most popular and widely used model in continuum framework is the Helfrich model that was proposed in 1973 [102]. In this model, the membrane is considered as a thin elastic shell that can bend such that at all the times the lipids remain aligned and normal to the membrane surface. In addition, this model presumes that the curvature of the membrane is much larger than the thickness of the bilayer [102]. Under these assumptions, Helfrich proposed an energy function for the membrane system that depends only on the mean and Gaussian curvatures of the membrane as [102]

$$W_{\text{Bending}} = \int_{\omega} 2\kappa H^2 + \kappa_G K dA, \tag{1}$$

where W is total strain energy of the membrane due to bending, H is the membrane mean curvature, K is the membrane Gaussian curvature, and κ and κ_G are the membrane properties which are called the bending and Gaussian modulii respectively. The integration in Eq. 1 is over the entire membrane surface area ω and dA is the area element. We describe the geometrical concepts of membrane curvature in Box. A.

3.2. Simulation techniques

From a mechanical perspective, cell membrane deformation can be characterized by balance laws for mass and momentum. Simplifying these mass and momentum governing equations in continuum framework results in partial differential equations (PDEs) [103]. To solve the PDEs, first step we need to define the constitutive relationship for membrane deformation such as Helfrich bending energy (Eq. 1). Other forms of suggested constitutive equations including the effects of proteins are presented in Sec. 4.

Besides the need for a constitutive equation, the derived PDEs from cell mechanics are usually higher order and highly nonlinear differential equations. Therefore, in most cases, analytical solution are not possible and the equations are often solved numerically. Over the last few decades, various computational approaches have been developed to solve the set of governing PDEs including the boundary value problem for axisymmetric coordinates [21,37,44,104,105], different finite

element methods [106–108], Monte Carlo methods [109–111], finite difference methods [112,113], and the phase field representation of the surface [114–116]. Each of these methods has its own advantage and disadvantage and depending on the complexity of the problem, one or more of them can be implemented.

A major challenge in modeling membrane protein interactions is identifying a constitutive relationship that captures the different levels of complexities associated with membrane protein interactions. In what follows, we discuss some of the popular models used for such purposes along with their applications. We then discuss where new constitutive relationships relationships are needed and how these can be experimentally parameterized.

4. Continuum elastic energy models of membrane-protein interaction

4.1. Spontaneous curvature model

In the spontaneous curvature (SC) model, it has been suggested that the interaction between proteins and surrounding lipids changes the local membrane properties particularly the preferred – called spontaneous – curvature of the membrane [18,117–119]. In this case, the induced spontaneous curvature is a parameter that reflects a possible asymmetry between the two leaflets of the bilayer. This can be the result of any membrane bending mechanisms such as phase separation of membrane proteins into distinct domains, amphipathic helix or conically shaped transmembrane protein insertion, protein scaffolding, or protein crowding (Fig. 5A). In reality, a combination of all these mechanisms can occur simultaneously and the local value of spontaneous curvature can then be interpreted as a single measure of the curvature-generating capability of the membrane-protein interaction [17,18]. In a continuum framework, the most common model for induced spontaneous curvature is the modified version of Helfrich energy (Eq. 1), given by [44,118,120,121]

$$W_{\mathrm{SC}} = \int_{\omega} 2\kappa(H - C)^2 + \kappa_G K dA, \tag{2}$$

where C is the spontaneous curvature and its effective strength depends on the membrane composition, temperature, the membrane thickness, the protein density, and the membrane area coverage by proteins [102,122].

Modeling the net effect of membrane-protein interaction as an induced spontaneous curvature (Eq. 2) has provided great insight into various aspects of membrane deformation, from vesiculation in caveolae and endosomal sorting complexes to cylindrical shapes of membrane endoplasmic reticulum (ER) [123–125]. By using the SC model, recent studies have shown for example how a line tension at a lipid phase boundary could drive scission in yeast endocytosis [21,126,127], or how a snapthrough transition from open U-shaped buds to closed Ω-shaped buds in Clathrin Mediated Endocytosis (CME) is regulated by membrane tension [37,44]. Furthermore, the experimentally observed change in membrane tension (spontaneous tension) in response to protein adsorption [128–130], can be explained in the context of the SC model [104,120,122]. The SC model has also been used to elucidate the role of varying membrane tension due to spontaneous curvature papers [104,120,122]. While the SC model has been very effective in capturing large scale deformations of the membrane, it doesn't take into account the protein density or the curvature induced by each protein.

Box A. Curvatures of surfaces

Let us consider the membrane as a two dimensional surface in a three dimensional Euclidean space (Fig. A3). At each point on the surface, there are two curvatures, κ_1 and κ_2, which characterize the shape of the surface [131,132]. These two curvatures are called principal curvatures and by the definition their values are the reciprocal of the radius of the osculating circle at the point (**P**) ($\kappa_1 = 1/R_1$ and $\kappa_2 = 1/R_2$ in Fig. A3) [131,132]. The values of these curvatures can be positive or negative. The curvature is positive if the curve turns in a same direction as normal vector to the surface (**n**), otherwise it is negative [131,132]. The average and the product of two principal curvatures give the mean (H) and the Gaussian (K) curvatures as [131,132]

$$H = \frac{\kappa_1 + \kappa_2}{2} \quad \text{and} \quad K = \kappa_1 \kappa_2. \tag{A.1}$$

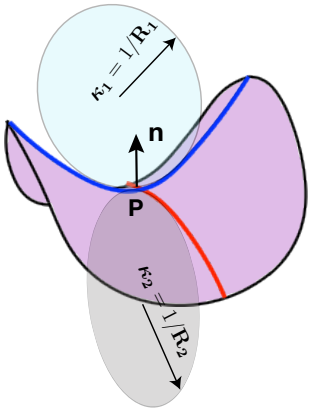

Figure A3. Principal curvatures of a surface.

For a rotationally symmetric surface as shown in Fig. A4, we can define the position of each point on the surface as a function of arc length (s) such as

$$\mathbf{r}(s) = r(s)\mathbf{e_r}(\theta) + z(s)\mathbf{k}, \tag{A.2}$$

where $r(s)$ is the radius from axis of revolution, $z(s)$ is the elevation from a base plane, and $(\mathbf{e_r}, \mathbf{e_\theta}, \mathbf{k})$ forms the coordinate basis. Since $r^2(s) + z^2(s) = 1$, we can define the angle ψ such that (Fig. A4)

$$\mathbf{a}_s = \cos(\psi)\mathbf{e_r} + \sin(\psi)\mathbf{k} \quad \text{and} \quad \mathbf{n} = -\sin(\psi)\mathbf{e_r} + \cos(\psi)\mathbf{k}, \tag{A.3}$$

where $\mathbf{a}_s$ and $\mathbf{n}$ are the unit tangent and normal vectors to the surface as shown in Fig. A4. We now can define the two principal curvatures as

$$\kappa_1 = \psi' \quad \text{and} \quad \kappa_2 = \frac{\sin(\psi)}{r}, \tag{A.4}$$

where $(\cdot)' = d(\cdot)/ds$ is the partial derivative with respect to the arc length. With having the two principal curvatures, the curvature deviator (D) in anisotropic condition is given by

$$D = \frac{1}{2}\left(\frac{\sin(\psi)}{r} - \psi'\right). \tag{A.5}$$

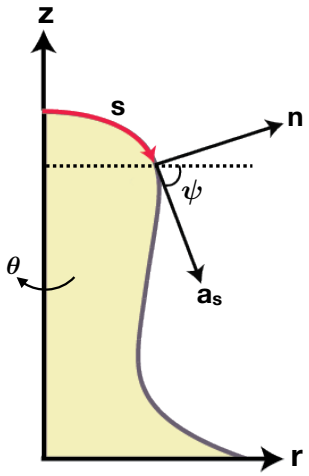

Figure A4. Axisymmetric coordinates with **z** as the axis of rotation.

4.2. Bilayer couple model

In order to go beyond an idealized single manifold description of a membrane, the Bilayer Couple model (BC) was proposed by Sheetz and Singer in 1974 [133]. The basic idea in this model is that each lipid molecule has a fixed area and there is no lipid exchange between the two leaflets of the bilayer. Thus, any asymmetrical protein insertions into the inner and outer surfaces of the membrane causes an area mismatch between the two leaflets. This mismatch creates in-plane compression in one leaflet and extension in the other, resulting in membrane deformation to release the induced stress (Fig. 5B) [18,134]. For a thin lipid bilayer with thickness (d), the area difference between the leaflets (ΔA) can be expressed in terms of the mean curvature (H) as

$$\Delta A = 2d \int_{\omega} H dA. \tag{3}$$

Here, instead of having a spontaneous curvature term in energy, a “hard" constraint on the area difference between the leaflets (Eq. 3) regulates the membrane curvature. This difference in the mechanism of curvature generation of SC and BC models distinguishes their predictions for the same membrane deformation [134]. For example, in membrane budding transition due to thermal expansion, the prediction of the SC model is that the shape transformation is discontinuous, while based on the BC model, there are pear-shaped structures that appear as intermediates and the transition of shapes is continuous [134].

4.3. Area difference elasticity model

In 1980, the Area Difference Elasticity (ADE) model was developed by Svetina *et.al*, [135,136] to combine both SC and BC models including the missing macroscopic details of membrane bending phenomena. To better explain the physics underlying this model, we consider a flat membrane that bends downward due to different protein concentrations on two sides of the membrane (Fig. 5C). This bending, based on the single sheet descriptions of the membrane in SC model, gives rise to the spontaneous curvature term in the energy equation (Eq. 2). However, if we treat each leaflet as an independent elastic plate – as was suggested in the BC model – we can then see that besides the curvature, the area of each monolayer will also change. For example, in Fig. 5C, the outer monolayer is stretched and the inner one is compressed. The energy associated with the membrane bending and this relative change in the monolayers areas is given by [134,137,138]

$$W_{\mathrm{ADE}} = \underbrace{\int_{\omega} 2\kappa(H-C)^2 + \kappa_G K dA}_{\text{Bending energy}} + \underbrace{\frac{\kappa_r}{2Ad^2}(\Delta A - \Delta A_0)^2}_{\text{Elastic stretching energy}}, \tag{4}$$

where κ_r is called the nonlocal membrane bending modulus, and A is the total surface area of the neutral plane. ΔA_0 and ΔA are the relaxed (initial) and the bent area differences between the membrane leaflets respectively ($\Delta A_0 = A_{0,\mathrm{out}} - A_{0,\mathrm{in}}$ and $\Delta A = A_{\mathrm{out}} - A_{\mathrm{in}}$, in which A_{out} is the area of the outer layer and A_{in} is the area of the inner layer). In Eq. 4, κ and κ_r are both in order of $K_a d^2$, where K_a is the area stretching modulus of the bilayer [134,138,139]. This means that in any membrane deformation, both the terms, the bending and the elastic stretching energies, are comparable and must be considered. Using the ADE model, researchers for the first time could numerically simulate the shape transformations of the human red blood cell from stomatocyte to discocyte and to echinocyte [139–142]. Also, using the ADE model the experimentally observed vesicles were mapped into a theoretical phase diagram, enabling theoreticians to predict in what regions or range of parameters, the vesicles may become unstable [134,137]. These predictions have been very useful for detecting unstable shapes, which is challenging to do experimentally.

Preprints (www.preprints.org) | NOT PEER-REVIEWED | Posted: 4 September 2018 doi:10.20944/preprints201809.0055.v1

Peer-reviewed version available at Biomolecules 2018, 8, 120; doi:10.3390/biom8040120

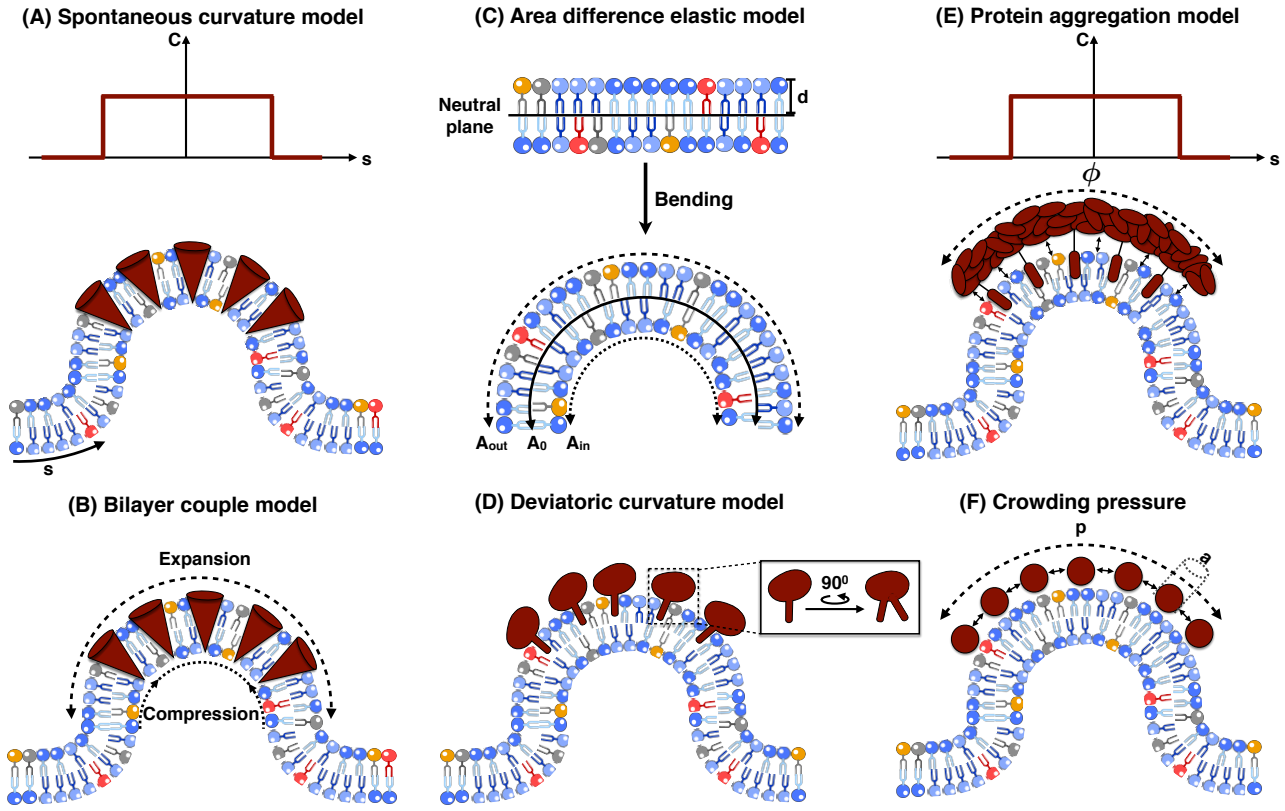

Figure 5. The mechanisms of membrane curvature generation due to protein interactions in different continuum elastic models. (A) Local protein interactions with membrane produces a spontaneous curvature filed. (B) The asymmetric insertion of conical proteins on one side of the membrane results in the expansion of the upper leaflet and compression of the lower leaflet. (C) The are of each membrane leaflet changes due to membrane bending. (D) Rotationally non-symmetric proteins generates anisotropic curvature. (E) Aggregated proteins on the membrane surface creates a spontaneous curvature filed and also have entropic interactions with the membrane. Here ϕ represents the relative density of the accumulated proteins. (F) The induced pressure (p) by crowding proteins drives membrane bending. a is the surface area occupied by one protein.

4.4. Deviatoric curvature model

In the SC model, the induced spontaneous curvature was assumed to be isotropic, same in both directions (see Box. A). However, not all proteins are rotationally symmetric and have intrinsically anisotropic structures such as banana shaped BIN-amphiphysin-Rvs (BAR) proteins (Fig. 5D) [143–145]. These proteins can produce different curvatures in different directions and this difference is required for the formation of nonspherical structures such as membrane tubular protrusions [146,146,147]. In order to take into account the anisotropic contribution of protein coats or inclusions in the continuum approach, Kralj-Iglic *et. al* proposed a Deviatoric Elasticity (DE) model [148]. In this model, each complex protein structure is simplified as a one-dimensional curve that lies on the membrane. The orientation and the position of the proteins in the plane of the membrane are important factors since an extra term is needed in the for adjusting the actual local curvature of the membrane to the intrinsic curvatures of the proteins [148,149]. The membrane-free energy that was suggested by the DE model is given as [148,150]

$$W_{\mathrm{DE}} = \int_{\omega} \underbrace{2\kappa(H-C)^2 + \kappa_{\mathrm{G}}K}_{\text{Bending energy}} + \underbrace{2\kappa(D-D_0)^2}_{\text{Deviatoric mismatch}}\, dA, \tag{5}$$

where D is the membrane curvature deviator and D_0 is the spontaneous membrane curvature deviator. Since the DE model was proposed, there have been many modeling efforts to explain how BAR proteins accumulation in membrane necks stabilize membrane tubular protrusions without any cytoskeleton supports [151–154]. Effectively, derivation of the Euler-Lagrange governing equations by a variational approach [155], provides a platform to systematically explore the impact of the induced stresses by anisotropic curvatures on the morphology of tubular structures [21].

4.5. Protein aggregation model

Aggregation of cytosolic proteins on the membrane surface or phase separation of bilayer proteins into specific domains have been observed in many biological processes [156–159]. This aggregation of proteins not only creates a concentration field on the membrane surface but also results in additional contributions to the membrane energy due to compositional heterogeneity and the entropic interactions of bulk proteins with the lipid bilayer (Fig. 5E) [160–162]. While the exact form of the free energy is still a matter of debate and has not been verified experimentally yet, a simple model based on thermodynamic arguments is given as [160,161,163],

$$W_{\mathrm{Aggregation}} = \int_{\omega} \underbrace{2\kappa(H-C)^2 + \kappa_{\mathrm{G}}K}_{\text{Bending energy}} + \underbrace{\frac{T}{a^2}(\phi\ln\phi + (1-\phi)\ln(1-\phi))}_{\text{Entropic energy}} + \underbrace{\frac{J}{2a^2}\phi(1-\phi)}_{\substack{\text{Energy due to protein}\\ \text{aggregation}}} + \underbrace{\frac{J}{4}(\nabla\phi)^2}_{\substack{\text{Energy penalty due}\\ \text{to compositional}\\ \text{heterogeneity}}} dA, \tag{6}$$

where T is the environment temperature, a is the surface area occupied by one protein, ϕ is the relative density of the proteins, and J is the aggregation potential. In Eq. 6, the first term is the conventional Helfrich bending energy with induced spontaneous curvature [102]. The second term represents the entropic contribution due to the thermal motion of proteins in the membrane [160,164]. The third term gives the aggregation energy, and the last term describes the energetic penalty for the spatial membrane composition gradient [160,163,164]. The suggested protein aggregation model mainly used for theoretical analysis of dynamic phase transitions of coupled membrane- proteins- cytoskeleton systems in membrane protrusions such as microvilli and filopodia [160,165–167]. This model also reveals one interesting fact that in addition to the induced deviatoric spontaneous curvature of the BAR domain proteins, the associated energy with their aggregation at membrane necks facilitates tubular structures stability. [154,168]. A major open question in the field is the relationship between protein density, size, and spontaneous curvature. Although current models use a linear proportionality [104,161,169], this choice of functions is critical in determining the energy.

4.6. Protein crowding

Protein crowding is a recently discovered curvature generating mechanism that has challenged some conventional paradigms about the role of involved molecular machinery in a robust cell shape change [34–36,170–172]. Stachowiak *et. al.* reported that confining a sufficiently high concentration of his-tagged Green Fluorescent Proteins (GFP) to a local region can deform the membrane into buds or tubules in the absence of any protein insertion into the lipid bilayer [35,170]. Furthermore, Snead *et. al.* showed that crowding among membrane-bound proteins can also drive membrane fission [34]. This paper

raises a controversial prediction that the large disordered domains of BAR domains proteins induce crowding pressure that promotes membrane fission instead of stabilizing the membrane [173]. Additionally, another set of experiments reported that the induced crowding pressure by a high concentration of cargo proteins on one side of the ER works as an obstacle, which opposes membrane bending and inhibits the vesiculation by coat protein complex II (COPII) [174–176].

The essence of the crowding mechanism is that the lateral collisions between the membrane-bound proteins on one side of the membrane generate a steric pressure that causes the membrane to bend away from the bulk proteins (Fig. 5F)[35,177,178]. As the density, the size or the mobility of the bound proteins increase, the induced steric pressure becomes larger, which results in a more significant membrane bending [35,36]. Modeling the free energy associated with protein crowding is more difficult because it profoundly depends on the specific composition of the underlying membrane as well as the lateral confinement of the membrane-bound proteins [179,180]. However, in a recent paper, a simple 2D hard-sphere gas model based on the Carnahan-Starling approximation has been proposed to describe the free energy of the crowding mechanism [35,181]. To better visualize it, let us consider a membrane that is crowded with different protein concentration on each side as shown in Fig. 5. If we model each protein as a hard-sphere gas particle that exerts certain pressure to the membrane surface, the work that is done by this pressure to bend the membrane according to the standard thermodynamics is given by [182]

$$W_{\text{Crowding}} = \int p_{\text{in}} dA_{\text{in}} + \int p_{\text{out}} dA_{\text{out}}, \tag{7}$$

where p_{in} and p_{out} are the induced steric pressure by the crowding proteins on the inner side and the outer side of the membrane respectively. This induced pressure (denoted by p here) for a 2D hard-sphere gas protein can be expressed as [180,183,184]

$$p = \frac{k_B T}{a} p_R(\phi), \tag{8}$$

where k_B is the Boltzmann constant and $p_R(\phi)$ is the reduced gas pressure depending on the relative density of the protein given as [184]

$$p_R(\phi) = \phi(1 + 2\phi \frac{1 - \frac{7}{16}\phi}{(1-\phi)^2}). \tag{9}$$

Eq. 9 is known as a 2D version of the Carnahan-Starling equation. Based on this equation, at low protein density, the reduced pressure is simply proportional to ϕ, but as the gas density increases, the non-linear terms play larger roles and should be considered.

4.7. Hydrophobic mismatch

Transmembrane proteins embedded in the cell membrane have a hydrophobic region that is in contact with the hydrophobic region (lipid acyl chain) of the lipid bilayer. Energetically, it is then favorable that both hydrophobic regions have approximately a same thickness in order to prevent the exposure of the hydrophobic surfaces to the hydrophilic environment. However, there are various proteins with different lengths in a single membrane [185,186]. On the other hand, one protein with a same length can be surrounded by lipid bilayers with different thicknesses [187,188]. This difference between thicknesses of hydrophobic regions of a transmembrane protein (d_p) and the lipid bilayer (d_l) is called hydrophobic mismatch. There are different adaptation mechanisms that either the protein or the bilayer can utilize in order to avoid

the energy cost of the hydrophobic mismatch [187,189]. For example, for positive ($d_l < d_p$) or negative ($d_l > d_p$) mismatch, the lipid bilayer can be stretched or compressed respectively to adjust the length of hydrophobic regions [190,191]. Another possibility is when the hydrophobic part of a transmembrane protein is too thick or too short as compared to the hydrophobic bilayer thickness. In this case, protein aggregation on the membrane or protein surface localization can efficiently minimize the exposed hydrophobic area [192,193]. Also, for proteins that have helices that are too long compared to the thickness of the membrane, helix tilt is one possible mechanism to reduce the protein effective hydrophobic length [187,194,195]. Several theoretical approaches have been developed to incorporate the energy cost and thermodynamic effects of membrane-protein interactions in term of hydrophobic mismatch [196–199].

Thus, in addition to the models described above, there are additional considerations to the energy that have been suggested by numerous studies such as higher order bending terms [132,200,201], lipid volume constraints [202], the impacts of a protein shape on membrane deformation [203], and the electrostatic energy between a membrane and proteins [204–207].

5. Future perspective and challenges

Although the models discussed above have provided insight into some fundamental questions about the molecular machinery of cell shape regulation, all of them have been developed based on simplifying assumptions that need to be revisited in the pursuit of closing the gap between experiment and theory. In order to achieve this goal, multidisciplinary efforts between physicists, mathematicians, engineers, and biologists are required to match different pieces of this cell biology puzzle.

Here, we highlight some current challenges that we believe must be considered in the next generation of continuum models.

- Membrane deformation is a dynamic process, surrounding fluid flow, thermal fluctuation, and diffusion of proteins actively regulate the shape of the membrane at each instance [11,169,208–212]. Currently, the models for membranes at mechanical equilibrium are quite well developed but the models for a dynamic process have not been as well-developed and the community must invest some effort in this aspect.
- In *vivo*, multiple mechanisms coupling membrane deformation and cytoskeletal remodeling are commonplace (Fig. 6A). Therefore, the models should be extended to include the dynamic effect and rearrangement of the actin cytoskeleton layer underneath of the membrane.
- Membrane deformation and protein absorption/rearrangement are often considered as two separate processes with little to no impact on each other. However, recent studies show that proteins can sense the membrane curvature (Fig. 6B). Therefore, indeed, there is a feedback loop between the protein distribution and the membrane configuration. While some models are discussed in [161,216–219], we still need more quantitative agreements between theory and experiment.
- Cell shape can control signal transduction at the plasma membrane, and on the other hands, intracellular signaling changes the membrane tension [220] (Fig. 6C). This coupling between the cell shape and the signaling network inside the cell should be further understood in terms of both quantitative experimental and theoretical biology.
- As discussed above, membrane deformation is a multiscale phenomena that results from the reorientation of lipids to large scale change in membrane curvature. This suggests the extension of available models toward multiscale models that could represent each biological process over multiple length scales [101,221].

Despite these challenges, with increasingly quantitative measurement techniques available experimentally, ease of access to high throughput computing systems, and interdisciplinary training the next generation of scientist leaders, the future of theoretical modeling of biological membranes and cellular membrane processes is brighter than ever.

Acknowledgments This work was supported by ARO W911NF-16-1-0411, ONR N00014-17-1-2628 grants to P.R. H.A. was supported by a fellowship from the Visible Molecular Cell Consortium (VMCC), a program between UCSD

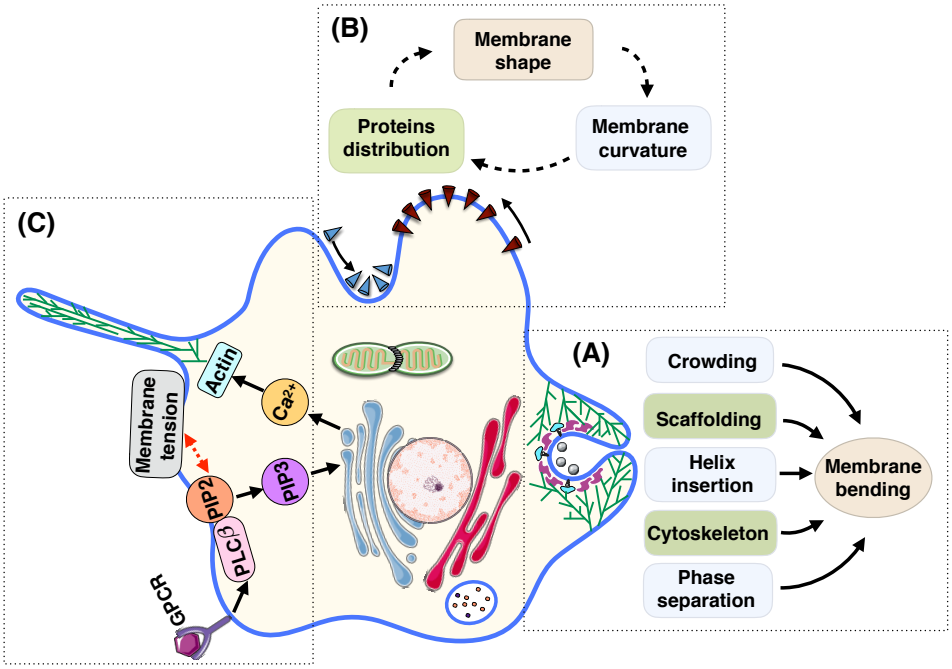

Figure 6. Perspective for the the future of theoretical models for membrane curvature generating mechanisms. (A) The coupling between membrane shape, membrane curvature, and membrane proteins distribution. The convex proteins (indicated with red cones) aggregate and flow toward the hill where the membrane curvature is negative (assuming the normal vector to the surface is outward). On the other hand, the concave proteins (represented by blue cones) accumulate and move toward the valley where the membrane curvature is large and positive [161]. (B) Various mechanisms are involved in trafficking including amphipathic helix insertion into the bilayer, protein scaffolding, cargo-receptor crowding, forces from actin polymerization, and lipid phase separation [213,214]. (C) The coupling between the formation of a filopodial protrusion and the intracellular signaling inside the cell [215].

and the Scripps Research Institute. The authors thank Miriam Bell and Allen Leung for their critical reading of the manuscript. Figures 1, 2, 3, and 4 used adapted content from Servier Medical Art powerpoint image bank (http://www.servier.com/Powerpoint-image-bank).

Author Contributions: H.A. and P.R. wrote the manuscript.

Conflicts of Interest: The authors declare no conflict of interest.

References

1. Mukherjee, S.; Maxfield, F.R. Role of membrane organization and membrane domains in endocytic lipid trafficking. *Traffic* **2000**, *1*, 203–211.
2. Gruenberg, J. The endocytic pathway: a mosaic of domains. *Nature reviews Molecular cell biology* **2001**, *2*, 721.
3. Westermann, B. Mitochondrial fusion and fission in cell life and death. *Nature reviews Molecular cell biology* **2010**, *11*, 872.
4. Van der Bliek, A.M.; Shen, Q.; Kawajiri, S. Mechanisms of mitochondrial fission and fusion. *Cold Spring Harbor perspectives in biology* **2013**, *5*, a011072.
5. Grafmuller, A.; Shillcock, J.; Lipowsky, R. The fusion of membranes and vesicles: pathway and energy barriers from dissipative particle dynamics. *Biophysical journal* **2009**, *96*, 2658–2675.
6. Jahn, R.; Fasshauer, D. Molecular machines governing exocytosis of synaptic vesicles. *Nature* **2012**, *490*, 201.

7. Reilly, G.C.; Engler, A.J. Intrinsic extracellular matrix properties regulate stem cell differentiation. *Journal of biomechanics* **2010**, *43*, 55–62.
8. Xiong, Y.; Rangamani, P.; Fardin, M.A.; Lipshtat, A.; Dubin-Thaler, B.; Rossier, O.; Sheetz, M.P.; Iyengar, R. Mechanisms controlling cell size and shape during isotropic cell spreading. *Biophysical journal* **2010**, *98*, 2136–2146.
9. Rangamani, P.; Fardin, M.A.; Xiong, Y.; Lipshtat, A.; Rossier, O.; Sheetz, M.P.; Iyengar, R. Signaling network triggers and membrane physical properties control the actin cytoskeleton-driven isotropic phase of cell spreading. *Biophysical journal* **2011**, *100*, 845–857.
10. Neves, S.R.; Tsokas, P.; Sarkar, A.; Grace, E.A.; Rangamani, P.; Taubenfeld, S.M.; Alberini, C.M.; Schaff, J.C.; Blitzer, R.D.; Moraru, I.I.; others. Cell shape and negative links in regulatory motifs together control spatial information flow in signaling networks. *Cell* **2008**, *133*, 666–680.
11. Rangamani, P.; Lipshtat, A.; Azeloglu, E.U.; Calizo, R.C.; Hu, M.; Ghassemi, S.; Hone, J.; Scarlata, S.; Neves, S.R.; Iyengar, R. Decoding information in cell shape. *Cell* **2013**, *154*, 1356–1369.
12. Bell, M.; Bartol, T.; Sejnowski, T.; Rangamani, P. Dendritic spine geometry and spine apparatus organization govern the spatiotemporal dynamics of calcium. *bioRxiv* **2018**, p. 386367.
13. Giardini, P.A.; Fletcher, D.A.; Theriot, J.A. Compression forces generated by actin comet tails on lipid vesicles. *Proceedings of the National Academy of Sciences* **2003**, *100*, 6493–6498.
14. Carlsson, A.E. Membrane bending by actin polymerization. *Current opinion in cell biology* **2018**, *50*, 1–7.
15. Kaksonen, M.; Toret, C.P.; Drubin, D.G. Harnessing actin dynamics for clathrin-mediated endocytosis. *Nature reviews Molecular cell biology* **2006**, *7*, 404.
16. McMahon, H.T.; Gallop, J.L. Membrane curvature and mechanisms of dynamic cell membrane remodelling. *Nature* **2005**, *438*, 590.
17. Zimmerberg, J.; Kozlov, M.M. How proteins produce cellular membrane curvature. *Nature reviews Molecular cell biology* **2006**, *7*, 9.
18. Argudo, D.; Bethel, N.P.; Marcoline, F.V.; Grabe, M. Continuum descriptions of membranes and their interaction with proteins: towards chemically accurate models. *Biochimica et Biophysica Acta (BBA)-Biomembranes* **2016**, *1858*, 1619–1634.
19. Kozlov, M.M.; Campelo, F.; Liska, N.; Chernomordik, L.V.; Marrink, S.J.; McMahon, H.T. Mechanisms shaping cell membranes. *Current opinion in cell biology* **2014**, *29*, 53–60.
20. Jenkins, J. Static equilibrium configurations of a model red blood cell. *Journal of mathematical biology* **1977**, *4*, 149–169.
21. Alimohamadi, H.; Vasan, R.; Hassinger, J.; Stachowiak, J.C.; Rangamani, P. The role of traction in membrane curvature generation. *Molecular Biology of the Cell* **2018**, *29*, 2024–2035.
22. Alimohamadi, H.; Vasan, R.; Hassinger, J.; Stachowiak, J.; Rangamani, P. The role of traction in membrane curvature generation. *Biophysical Journal* **2018**, *114*, 600a.
23. Guven, J. Membrane geometry with auxiliary variables and quadratic constraints. *Journal of Physics A: Mathematical and General* **2004**, *37*, L313.
24. Aridor, M.; Bannykh, S.I.; Rowe, T.; Balch, W.E. Sequential coupling between COPII and COPI vesicle coats in endoplasmic reticulum to Golgi transport. *The Journal of cell biology* **1995**, *131*, 875–893.
25. Davies, K.M.; Anselmi, C.; Wittig, I.; Faraldo-Gomez, J.D.; Kuhlbrandt, W. Structure of the yeast F1Fo-ATP synthase dimer and its role in shaping the mitochondrial cristae. *Proceedings of the National Academy of Sciences* **2012**, *109*, 13602–13607.
26. Landau, E.M.; Rosenbusch, J.P. Lipidic cubic phases: a novel concept for the crystallization of membrane proteins. *Proceedings of the National Academy of Sciences* **1996**, *93*, 14532–14535.
27. Schmidt, N.W.; Mishra, A.; Wang, J.; DeGrado, W.F.; Wong, G.C. Influenza virus A M2 protein generates negative Gaussian membrane curvature necessary for budding and scission. *Journal of the American Chemical Society* **2013**, *135*, 13710–13719.
28. Gallop, J.L.; Jao, C.C.; Kent, H.M.; Butler, P.J.G.; Evans, P.R.; Langen, R.; McMahon, H.T. Mechanism of endophilin N-BAR domain-mediated membrane curvature. *The EMBO journal* **2006**, *25*, 2898–2910.
29. Pucadyil, T.J.; Schmid, S.L. Conserved functions of membrane active GTPases in coated vesicle formation. *Science* **2009**, *325*, 1217–1220.
30. Lee, M.C.; Orci, L.; Hamamoto, S.; Futai, E.; Ravazzola, M.; Schekman, R. Sar1p N-terminal helix initiates membrane curvature and completes the fission of a COPII vesicle. *Cell* **2005**, *122*, 605–617.

31. Campelo, F.; McMahon, H.T.; Kozlov, M.M. The hydrophobic insertion mechanism of membrane curvature generation by proteins. *Biophysical journal* **2008**, *95*, 2325–2339.
32. Karotki, L.; Huiskonen, J.T.; Stefan, C.J.; Ziolkowska, N.E.; Roth, R.; Surma, M.A.; Krogan, N.J.; Emr, S.D.; Heuser, J.; Grunewald, K.; others. Eisosome proteins assemble into a membrane scaffold. *J Cell Biol* **2011**, *195*, 889–902.
33. Daumke, O.; Roux, A.; Haucke, V. BAR domain scaffolds in dynamin-mediated membrane fission. *Cell* **2014**, *156*, 882–892.
34. Snead, W.T.; Hayden, C.C.; Gadok, A.K.; Zhao, C.; Lafer, E.M.; Rangamani, P.; Stachowiak, J.C. Membrane fission by protein crowding. *Proceedings of the National Academy of Sciences* **2017**, *114*, E3258–E3267.
35. Stachowiak, J.C.; Schmid, E.M.; Ryan, C.J.; Ann, H.S.; Sasaki, D.Y.; Sherman, M.B.; Geissler, P.L.; Fletcher, D.A.; Hayden, C.C. Membrane bending by protein–protein crowding. *Nature cell biology* **2012**, *14*, 944.
36. Busch, D.J.; Houser, J.R.; Hayden, C.C.; Sherman, M.B.; Lafer, E.M.; Stachowiak, J.C. Intrinsically disordered proteins drive membrane curvature. *Nature communications* **2015**, *6*, 7875.
37. Hassinger, J.E.; Oster, G.; Drubin, D.G.; Rangamani, P. Design principles for robust vesiculation in clathrin-mediated endocytosis. *Proceedings of the National Academy of Sciences* **2017**, *114*, E1118–E1127.
38. Shen, Z.; Ye, H.; Li, Y. Understanding receptor-mediated endocytosis of elastic nanoparticles through coarse grained molecular dynamic simulation. *Physical Chemistry Chemical Physics* **2018**.
39. Bobrovska, N.; Gozdz, W.; Kralj-Iglic, V.; Iglic, A. On the role of anisotropy of membrane components in formation and stabilization of tubular structures in multicomponent membranes. *PloS one* **2013**, *8*, e73941.
40. Bahrami, A.H.; Hummer, G. Formation and stability of lipid membrane nanotubes. *ACS nano* **2017**, *11*, 9558–9565.
41. Torbati, M.; Lele, T.P.; Agrawal, A. Ultradonut topology of the nuclear envelope. *Proceedings of the National Academy of Sciences* **2016**, *113*, 11094–11099.
42. Liang, X.; Zu, Y.; Cao, Y.P.; Yang, C. A dual-scale model for the caveolin-mediated vesiculation. *Soft Matter* **2013**, *9*, 7981–7987.
43. Woo, H.J.; Wallqvist, A. Spontaneous buckling of lipid bilayer and vesicle budding induced by antimicrobial peptide magainin 2: a coarse-grained simulation study. *The journal of physical chemistry B* **2011**, *115*, 8122–8129.
44. Walani, N.; Torres, J.; Agrawal, A. Endocytic proteins drive vesicle growth via instability in high membrane tension environment. *Proceedings of the National Academy of Sciences* **2015**, p. 201418491.
45. Weichsel, J.; Geissler, P.L. The more the tubular: dynamic bundling of actin filaments for membrane tube formation. *PLoS computational biology* **2016**, *12*, e1004982.
46. Beltran-Heredia, E.; Almendro-Vedia, V.G.; Monroy, F.; Cao, F.J. Modeling the Mechanics of Cell Division: Influence of Spontaneous Membrane Curvature, Surface Tension, and Osmotic Pressure. *Frontiers in physiology* **2017**, *8*, 312.
47. Markvoort, A.J.; Smeijers, A.; Pieterse, K.; van Santen, R.; Hilbers, P. Lipid-based mechanisms for vesicle fission. *The Journal of Physical Chemistry B* **2007**, *111*, 5719–5725.
48. Shi, Y. A glimpse of structural biology through X-ray crystallography. *Cell* **2014**, *159*, 995–1014.
49. Hsia, C.Y.; Richards, M.J.; Daniel, S. A review of traditional and emerging methods to characterize lipid–protein interactions in biological membranes. *Analytical Methods* **2015**, *7*, 7076–7094.
50. Marion, D. An introduction to biological NMR spectroscopy. *Molecular and Cellular Proteomics* **2013**, pp. mcp–O113.
51. Emsley, J.W.; Feeney, J.; Sutcliffe, L.H. *High resolution nuclear magnetic resonance spectroscopy*; Vol. 2, Elsevier, 2013.
52. Betzig, E.; Patterson, G.H.; Sougrat, R.; Lindwasser, O.W.; Olenych, S.; Bonifacino, J.S.; Davidson, M.W.; Lippincott-Schwartz, J.; Hess, H.F. Imaging intracellular fluorescent proteins at nanometer resolution. *Science* **2006**, *313*, 1642–1645.
53. Gao, L.; Shao, L.; Higgins, C.D.; Poulton, J.S.; Peifer, M.; Davidson, M.W.; Wu, X.; Goldstein, B.; Betzig, E. Noninvasive imaging beyond the diffraction limit of 3D dynamics in thickly fluorescent specimens. *Cell* **2012**, *151*, 1370–1385.
54. Bozzola, J.J.; Russell, L.D. *Electron microscopy: principles and techniques for biologists*; Jones and Bartlett Learning, 1999.
55. Stephens, D.J.; Allan, V.J. Light microscopy techniques for live cell imaging. *Science* **2003**, *300*, 82–86.
56. De Vries, A.H.; Mark, A.E.; Marrink, S.J. Molecular dynamics simulation of the spontaneous formation of a small DPPC vesicle in water in atomistic detail. *Journal of the American Chemical Society* **2004**, *126*, 4488–4489.
57. Marcoline, F.V.; Bethel, N.; Guerriero, C.J.; Brodsky, J.L.; Grabe, M. Membrane protein properties revealed through data-rich electrostatics calculations. *Structure* **2015**, *23*, 1526–1537.
58. MacCallum, J.L.; Bennett, W.D.; Tieleman, D.P. Partitioning of amino acid side chains into lipid bilayers: results from computer simulations and comparison to experiment. *The Journal of general physiology* **2007**, *129*, 371–377.

59. Du, Q.; Liu, C.; Wang, X. Simulating the deformation of vesicle membranes under elastic bending energy in three dimensions. *Journal of Computational Physics* **2006**, *212*, 757–777.
60. Chabanon, M.; Rangamani, P. Gaussian curvature directs the distribution of spontaneous curvature on bilayer membrane necks. *Soft matter* **2018**, *14*, 2281–2294.
61. Muller, M.; Katsov, K.; Schick, M. Biological and synthetic membranes: What can be learned from a coarse-grained description? *Physics Reports* **2006**, *434*, 113–176.
62. Noid, W.; Chu, J.W.; Ayton, G.S.; Krishna, V.; Izvekov, S.; Voth, G.A.; Das, A.; Andersen, H.C. The multiscale coarse-graining method. I. A rigorous bridge between atomistic and coarse-grained models. *The Journal of chemical physics* **2008**, *128*, 244114.
63. Alimohamadi, H.; Ovryn, B.; Rangamani, P. Protein-Mediated Beads-on-a-String Structure Formation Along Membrane Nanotubes in Live Cells. *Biophysical Journal* **2018**, *114*, 392a.
64. Cuvelier, D.; Derenyi, I.; Bassereau, P.; Nassoy, P. Coalescence of membrane tethers: experiments, theory, and applications. *Biophysical journal* **2005**, *88*, 2714–2726.
65. Vasan, R.; Hassinger, J.; Alimohamadi, H.; Drubin, D.; Rangamani, P. Energetics and Stability of Neck Formation in Yeast and Mammalian Endocytosis. *Biophysical Journal* **2018**, *114*, 281a.
66. Darnell, J.E.; Lodish, H.F.; Baltimore, D.; others. *Molecular cell biology*; Vol. 2, Scientific American Books New York, 1990.
67. Stillwell, W. *An introduction to biological membranes: from bilayers to rafts*; Newnes, 2013.
68. Cevc, G.; Marsh, D. *Phospholipid bilayers: physical principles and models*; Wiley, 1987.
69. Terzi, M.M.; Deserno, M. Lipid Membranes: From Self-assembly to Elasticity. In *The Role of Mechanics in the Study of Lipid Bilayers*; Springer, 2018; pp. 105–166.
70. Guidotti, G. The composition of biological membranes. *Archives of internal medicine* **1972**, *129*, 194–201.
71. Yeagle, P.L. *The structure of biological membranes*; CRC press, 2011.
72. Watson, H. Biological membranes. *Essays in biochemistry* **2015**, *59*, 43–69.
73. Schulz, G.E.; Schirmer, R.H. *Principles of protein structure*; Springer Science and Business Media, 2013.
74. Albersheim, P.; Anderson-Prouty, A.J. Carbohydrates, proteins, cell surfaces, and the biochemistry of pathogenesis. *Annual Review of Plant Physiology* **1975**, *26*, 31–52.
75. Jain, M.K.; Wagner, R.C.; others. Introduction to biological membranes. Technical report, Wiley New York, 1988.
76. Singer, S.J.; Nicolson, G.L. The fluid mosaic model of the structure of cell membranes. *Science* **1972**, *175*, 720–731.
77. Lodish, H.; Berk, A.; Zipursky, S.L.; Matsudaira, P.; Baltimore, D.; Darnell, J.; others. *Molecular cell biology*; Vol. 3, WH Freeman New York, 1995.
78. White, A.; Handler, P.; Smith, E.; Stetten Jr, D.; others. Principles of biochemistry. *Principles of Biochemistry.* **1959**, *2*.
79. Hong, H.; Tamm, L.K. Elastic coupling of integral membrane protein stability to lipid bilayer forces. *Proceedings of the National Academy of Sciences* **2004**, *101*, 4065–4070.
80. Lee, A.G. How lipids affect the activities of integral membrane proteins. *Biochimica et Biophysica Acta (BBA)-Biomembranes* **2004**, *1666*, 62–87.
81. Rangamani, P.; Steigmann, D. Variable tilt on lipid membranes. *Proc. R. Soc. A* **2014**, *470*, 20140463.
82. Phillips, R.; Ursell, T.; Wiggins, P.; Sens, P. Emerging roles for lipids in shaping membrane-protein function. *Nature* **2009**, *459*, 379.
83. Ray, S.; Kassan, A.; Busija, A.R.; Rangamani, P.; Patel, H.H. The plasma membrane as a capacitor for energy and metabolism. *American Journal of Physiology-Cell Physiology* **2016**, *310*, C181–C192.
84. Seaton, B.A.; Roberts, M.F. Peripheral membrane proteins. In *Biological Membranes*; Springer, 1996; pp. 355–403.
85. Benga, G. Protein-lipid interactions in biological membranes. In *Structure and Properties of Cell Membrane Structure and Properties of Cell Membranes*; CRC Press, 2017; pp. 167–196.
86. Tamm, L.K. *Protein-lipid interactions: from membrane domains to cellular networks*; John Wiley and Sons, 2006.
87. Garber, E.A.; Margoliash, E. Interaction of cytochrome c with cytochrome c oxidase: an understanding of the high-to low-affinity transition. *Biochimica et Biophysica Acta (BBA)-Bioenergetics* **1990**, *1015*, 279–287.
88. Day, E.D. Myelin basic protein. In *Contemporary topics in molecular immunology*; Springer, 1981; pp. 1–39.
89. Singer, S. The molecular organization of membranes. *Annual review of biochemistry* **1974**, *43*, 805–833.
90. Sharon, N.; Lis, H. Glycoproteins: structure and function. *Glycosciences: status and perspectives* **1996**, pp. 133–162.
91. Shylaja, M.; Seshadri, H. Glycoproteins: an overview. *Biochemical Education* **1989**, *17*, 170–178.

92. Wittmann, V. Glycoproteins: properties. In *Glycoscience*; Springer, 2008; pp. 1771–1793.
93. Nettleship, J.E. Structural biology of glycoproteins. In *Glycosylation*; InTech, 2012.
94. Easton, R.; Leader, T. Glycosylation of proteins–structure, function and analysis. *Life Sci Tech Bull* **2011**, *60*, 1–5.
95. Ramakrishnan, N.; Kumar, P.S.; Radhakrishnan, R. Mesoscale computational studies of membrane bilayer remodeling by curvature-inducing proteins. *Physics reports* **2014**, *543*, 1–60.
96. Canham, P.B. The minimum energy of bending as a possible explanation of the biconcave shape of the human red blood cell. *Journal of theoretical biology* **1970**, *26*, 61–81.
97. Safran, S. *Statistical thermodynamics of surfaces, interfaces, and membranes*; CRC Press, 2018.
98. Tobias, D.J.; Tu, K.; Klein, M.L. Atomic-scale molecular dynamics simulations of lipid membranes. *Current Opinion in Colloid & Interface Science* **1997**, *2*, 15–26.
99. Tieleman, D.P.; Marrink, S.J.; Berendsen, H.J. A computer perspective of membranes: molecular dynamics studies of lipid bilayer systems. *Biochimica et Biophysica Acta (BBA)-Reviews on Biomembranes* **1997**, *1331*, 235–270.
100. Lindahl, E.; Sansom, M.S. Membrane proteins: molecular dynamics simulations. *Current opinion in structural biology* **2008**, *18*, 425–431.
101. Chabanon, M.; Stachowiak, J.C.; Rangamani, P. Systems biology of cellular membranes: a convergence with biophysics. *Wiley Interdisciplinary Reviews: Systems Biology and Medicine* **2017**, *9*, e1386.
102. Helfrich, W. Elastic properties of lipid bilayers: theory and possible experiments. *Zeitschrift für Naturforschung C* **1973**, *28*, 693–703.
103. Sauer, R.A. On the computational modeling of lipid bilayers using thin-shell theory. In *The Role of Mechanics in the Study of Lipid Bilayers*; Springer, 2018; pp. 221–286.
104. Alimohamadi, H.; Ovryn, B.; Rangamani, P. Protein aggregation and membrane bending govern nanotube morphology. *bioRxiv* **2018**, p. 373811.
105. Agrawal, A.; Steigmann, D.J. Boundary-value problems in the theory of lipid membranes. *Continuum Mechanics and Thermodynamics* **2009**, *21*, 57–82.
106. Laadhari, A.; Saramito, P.; Misbah, C. An adaptive finite element method for the modeling of the equilibrium of red blood cells. *International Journal for Numerical Methods in Fluids* **2016**, *80*, 397–428.
107. Sauer, R.A.; Duong, T.X.; Mandadapu, K.K.; Steigmann, D.J. A stabilized finite element formulation for liquid shells and its application to lipid bilayers. *Journal of Computational Physics* **2017**, *330*, 436–466.
108. Duong, T.X.; Roohbakhshan, F.; Sauer, R.A. A new rotation-free isogeometric thin shell formulation and a corresponding continuity constraint for patch boundaries. *Computer Methods in Applied Mechanics and Engineering* **2017**, *316*, 43–83.
109. Ramakrishnan, N.; Kumar, P.S.; Ipsen, J.H. Monte Carlo simulations of fluid vesicles with in-plane orientational ordering. *Physical Review E* **2010**, *81*, 041922.
110. Guan, X.; Ma, M.; Gan, Z.; Xu, Z.; Li, B. Hybrid Monte Carlo and continuum modeling of electrolytes with concentration-induced dielectric variations. *Physical Review E* **2016**, *94*, 053312.
111. Sreeja, K.; Ipsen, J.H.; Kumar, P.S. Monte Carlo simulations of fluid vesicles. *Journal of Physics: Condensed Matter* **2015**, *27*, 273104.
112. Lau, C.; Brownell, W.E.; Spector, A.A. Internal forces, tension and energy density in tethered cellular membranes. *Journal of biomechanics* **2012**, *45*, 1328–1331.
113. Gu, R.; Wang, X.; Gunzburger, M. Simulating vesicle–substrate adhesion using two phase field functions. *Journal of Computational Physics* **2014**, *275*, 626–641.
114. Banham, T.; Li, B.; Zhao, Y. Pattern formation by phase-field relaxation of bending energy with fixed surface area and volume. *Physical Review E* **2014**, *90*, 033308.
115. Du, Q.; Wang, X. Convergence of numerical approximations to a phase field bending elasticity model of membrane deformations **2006**.
116. Zhang, J.; Das, S.; Du, Q. A phase field model for vesicle–substrate adhesion. *Journal of Computational Physics* **2009**, *228*, 7837–7849.
117. Arkhipov, A.; Yin, Y.; Schulten, K. Four-scale description of membrane sculpting by BAR domains. *Biophysical journal* **2008**, *95*, 2806–2821.
118. Steigmann, D. Fluid films with curvature elasticity. *Archive for Rational Mechanics and Analysis* **1999**, *150*, 127–152.

119. Kishimoto, T.; Sun, Y.; Buser, C.; Liu, J.; Michelot, A.; Drubin, D.G. Determinants of endocytic membrane geometry, stability, and scission. *Proceedings of the National Academy of Sciences* **2011**, p. 201113413.
120. Rangamani, P.; Mandadap, K.K.; Oster, G. Protein-induced membrane curvature alters local membrane tension. *Biophysical journal* **2014**, *107*, 751–762.
121. Agrawal, A.; Steigmann, D.J. Modeling protein-mediated morphology in biomembranes. *Biomechanics and modeling in mechanobiology* **2009**, *8*, 371.
122. Lipowsky, R. Spontaneous tubulation of membranes and vesicles reveals membrane tension generated by spontaneous curvature. *Faraday discussions* **2013**, *161*, 305–331.
123. Sens, P.; Turner, M.S. Theoretical model for the formation of caveolae and similar membrane invaginations. *Biophysical journal* **2004**, *86*, 2049–2057.
124. Rozycki, B.; Boura, E.; Hurley, J.H.; Hummer, G. Membrane-elasticity model of Coatless vesicle budding induced by ESCRT complexes. *PLoS computational biology* **2012**, *8*, e1002736.
125. Hu, J.; Shibata, Y.; Voss, C.; Shemesh, T.; Li, Z.; Coughlin, M.; Kozlov, M.M.; Rapoport, T.A.; Prinz, W.A. Membrane proteins of the endoplasmic reticulum induce high-curvature tubules. *Science* **2008**, *319*, 1247–1250.
126. Liu, J.; Sun, Y.; Drubin, D.G.; Oster, G.F. The mechanochemistry of endocytosis. *PLoS biology* **2009**, *7*, e1000204.
127. Liu, J.; Kaksonen, M.; Drubin, D.G.; Oster, G. Endocytic vesicle scission by lipid phase boundary forces. *Proceedings of the National Academy of Sciences* **2006**, *103*, 10277–10282.
128. Faris, M.E.A.; Lacoste, D.; Pécréaux, J.; Joanny, J.F.; Prost, J.; Bassereau, P. Membrane tension lowering induced by protein activity. *Physical review letters* **2009**, *102*, 038102.
129. Manneville, J.B.; Bassereau, P.; Ramaswamy, S.; Prost, J. Active membrane fluctuations studied by micropipet aspiration. *Physical Review E* **2001**, *64*, 021908.
130. Shi, Z.; Graber, Z.T.; Baumgart, T.; Stone, H.A.; Cohen, A.E. Cell membranes resist flow. *bioRxiv* **2018**, p. 290643.
131. Spivak, M.D. *A comprehensive introduction to differential geometry*; Publish or perish, 1970.
132. Deserno, M. Fluid lipid membranes: From differential geometry to curvature stresses. *Chemistry and physics of lipids* **2015**, *185*, 11–45.
133. Sheetz, M.P.; Singer, S. Biological membranes as bilayer couples. A molecular mechanism of drug-erythrocyte interactions. *Proceedings of the National Academy of Sciences* **1974**, *71*, 4457–4461.
134. Miao, L.; Seifert, U.; Wortis, M.; Dobereiner, H.G. Budding transitions of fluid-bilayer vesicles: the effect of area-difference elasticity. *Physical Review E* **1994**, *49*, 5389.
135. Svetina, S.; Brumen, M.; Zeks, B. Lipid bilayer elasticity and the bilayer couple interpretation of red-cell shape transformations and lysis. *Studia Biophysica* **1985**, *110*, 177–184.
136. Svetina, S.; Zeks, B. Membrane bending energy and shape determination of phospholipid vesicles and red blood cells. *European biophysics journal* **1989**, *17*, 101–111.
137. Dobereiner, H.G.; Evans, E.; Kraus, M.; Seifert, U.; Wortis, M. Mapping vesicle shapes into the phase diagram: A comparison of experiment and theory. *Physical Review E* **1997**, *55*, 4458.
138. Bozic, B.; Svetina, S.; Zeks, B.; Waugh, R. Role of lamellar membrane structure in tether formation from bilayer vesicles. *Biophysical journal* **1992**, *61*, 963–973.
139. Waugh, R.E. Elastic energy of curvature-driven bump formation on red blood cell membrane. *Biophysical journal* **1996**, *70*, 1027–1035.
140. Mukhopadhyay, R.; Lim, H.G.; Wortis, M. Echinocyte shapes: bending, stretching, and shear determine spicule shape and spacing. *Biophysical Journal* **2002**, *82*, 1756–1772.
141. HW, G.L.; Wortis, M.; Mukhopadhyay, R. Stomatocyte–discocyte–echinocyte sequence of the human red blood cell: Evidence for the bilayer–couple hypothesis from membrane mechanics. *Proceedings of the National Academy of Sciences* **2002**, *99*, 16766–16769.
142. Svetina, S.; Kuzman, D.; Waugh, R.E.; Ziherl, P.; Zeks, B. The cooperative role of membrane skeleton and bilayer in the mechanical behaviour of red blood cells. *Bioelectrochemistry* **2004**, *62*, 107–113.
143. Peter, B.J.; Kent, H.M.; Mills, I.G.; Vallis, Y.; Butler, P.J.G.; Evans, P.R.; McMahon, H.T. BAR domains as sensors of membrane curvature: the amphiphysin BAR structure. *Science* **2004**, *303*, 495–499.

144. Schweitzer, Y.; Kozlov, M.M. Membrane-mediated interaction between strongly anisotropic protein scaffolds. *PLoS computational biology* **2015**, *11*, e1004054.
145. Simunovic, M.; Prevost, C.; Callan-Jones, A.; Bassereau, P. Physical basis of some membrane shaping mechanisms. *Phil. Trans. R. Soc. A* **2016**, *374*, 20160034.
146. Frost, A.; Perera, R.; Roux, A.; Spasov, K.; Destaing, O.; Egelman, E.H.; De Camilli, P.; Unger, V.M. Structural basis of membrane invagination by F-BAR domains. *Cell* **2008**, *132*, 807–817.
147. Shimada, A.; Niwa, H.; Tsujita, K.; Suetsugu, S.; Nitta, K.; Hanawa-Suetsugu, K.; Akasaka, R.; Nishino, Y.; Toyama, M.; Chen, L.; others. Curved EFC/F-BAR-domain dimers are joined end to end into a filament for membrane invagination in endocytosis. *Cell* **2007**, *129*, 761–772.
148. Kralj-Iglic, V.; Svetina, S.; Zekz, B. Shapes of bilayer vesicles with membrane embedded molecules. *European biophysics journal* **1996**, *24*, 311–321.
149. Fournier, J. Nontopological saddle-splay and curvature instabilities from anisotropic membrane inclusions. *Physical review letters* **1996**, *76*, 4436.
150. Kralj-Iglic, V.; Heinrich, V.; Svetina, S.; Zeks, B. Free energy of closed membrane with anisotropic inclusions. *The European Physical Journal B-Condensed Matter and Complex Systems* **1999**, *10*, 5–8.
151. Kralj-Iglic, V.; Remskar, M.; Vidmar, G.; Fosnaric, M.; Iglic, A. Deviatoric elasticity as a possible physical mechanism explaining collapse of inorganic micro and nanotubes. *Physics Letters A* **2002**, *296*, 151–155.
152. Iglic, A.; Hagerstrand, H.; Veranic, P.; Plemenitas, A.; Kralj-Iglic, V. Curvature-induced accumulation of anisotropic membrane components and raft formation in cylindrical membrane protrusions. *Journal of Theoretical Biology* **2006**, *240*, 368–373.
153. Kabaso, D.; Bobrovska, N.; Gozdz, W.; Gov, N.; Kralj-Iglic, V.; Veranic, P.; Iglic, A. On the role of membrane anisotropy and BAR proteins in the stability of tubular membrane structures. *Journal of biomechanics* **2012**, *45*, 231–238.
154. Kabaso, D.; Gongadze, E.; Elter, P.; Van Rienen, U.; Gimsa, J.; Kralj-Iglic, V.; Iglic, A. Attachment of rod-like (BAR) proteins and membrane shape. *Mini reviews in medicinal chemistry* **2011**, *11*, 272–282.
155. Walani, N.; Torres, J.; Agrawal, A. Anisotropic spontaneous curvatures in lipid membranes. *Physical Review E* **2014**, *89*, 062715.
156. Reynwar, B.J.; Illya, G.; Harmandaris, V.A.; Müller, M.M.; Kremer, K.; Deserno, M. Aggregation and vesiculation of membrane proteins by curvature-mediated interactions. *Nature* **2007**, *447*, 461.
157. Tourdot, R.W.; Ramakrishnan, N.; Radhakrishnan, R. Defining the free-energy landscape of curvature-inducing proteins on membrane bilayers. *Physical Review E* **2014**, *90*, 022717.
158. Shi, Z.; Baumgart, T. Dynamics and instabilities of lipid bilayer membrane shapes. *Advances in colloid and interface science* **2014**, *208*, 76–88.
159. Shnyrova, A.V.; Frolov, V.A.; Zimmerberg, J. Domain-driven morphogenesis of cellular membranes. *Current Biology* **2009**, *19*, R772–R780.
160. Veksler, A.; Gov, N.S. Phase transitions of the coupled membrane-cytoskeleton modify cellular shape. *Biophysical journal* **2007**, *93*, 3798–3810.
161. Gov, N. Guided by curvature: shaping cells by coupling curved membrane proteins and cytoskeletal forces. *Phil. Trans. R. Soc. B* **2018**, *373*, 20170115.
162. Gil, T.; Ipsen, J.H.; Mouritsen, O.G.; Sabra, M.C.; Sperotto, M.M.; Zuckermann, M.J. Theoretical analysis of protein organization in lipid membranes. *Biochimica et Biophysica Acta (BBA)-Reviews on Biomembranes* **1998**, *1376*, 245–266.
163. Givli, S.; Giang, H.; Bhattacharya, K. Stability of multicomponent biological membranes. *SIAM Journal on Applied Mathematics* **2012**, *72*, 489–511.
164. Katz, S.; Givli, S. Curvature-Induced Spatial Ordering of Composition in Lipid Membranes. *Computational and mathematical methods in medicine* **2017**, *2017*.
165. Kabaso, D.; Shlomovitz, R.; Schloen, K.; Stradal, T.; Gov, N.S. Theoretical model for cellular shapes driven by protrusive and adhesive forces. *PLoS computational biology* **2011**, *7*, e1001127.
166. Shlomovitz, R.; Gov, N. Exciting cytoskeleton-membrane waves. *Physical Review E* **2008**, *78*, 041911.
167. Orly, G.; Naoz, M.; Gov, N. Physical model for the geometry of actin-based cellular protrusions. *Biophysical journal* **2014**, *107*, 576–587.
168. Kabaso, D.; Gongadze, E.; Jorgacevski, J.; Kreft, M.; Rienen, U.; Zorec, R.; Iglic, A. Exploring the binding dynamics of BAR proteins. *Cellular and molecular biology letters* **2011**, *16*, 398.

169. Agrawal, A.; Steigmann, D.J. A model for surface diffusion of trans-membrane proteins on lipid bilayers. *Zeitschrift für angewandte Mathematik und Physik* **2011**, *62*, 549.
170. Stachowiak, J.C.; Hayden, C.C.; Sasaki, D.Y. Steric confinement of proteins on lipid membranes can drive curvature and tubulation. *Proceedings of the National Academy of Sciences* **2010**, *107*, 7781–7786.
171. Chen, Z.; Atefi, E.; Baumgart, T. Membrane shape instability induced by protein crowding. *Biophysical journal* **2016**, *111*, 1823–1826.
172. Callan-Jones, A.; Bassereau, P. Curvature-driven membrane lipid and protein distribution. *Current Opinion in Solid State and Materials Science* **2013**, *17*, 143–150.
173. Snead, W.; Zeno, W.; Kago, G.; Perkins, R.; Richter, J.B.; Lafer, E.; Stachowiak, J. BAR scaffolds drive membrane fission by crowding disordered domains. *bioRxiv* **2018**, p. 276147.
174. Copic, A.; Latham, C.F.; Horlbeck, M.A.; D'Arcangelo, J.G.; Miller, E.A. ER cargo properties specify a requirement for COPII coat rigidity mediated by Sec13p. *Science* **2012**, *335*, 1359–1362.
175. DArcangelo, J.G.; Crissman, J.; Pagant, S.; Copic, A.; Latham, C.F.; Snapp, E.L.; Miller, E.A. Traffic of p24 proteins and COPII coat composition mutually influence membrane scaffolding. *Current Biology* **2015**, *25*, 1296–1305.
176. Brandizzi, F.; Barlowe, C. Organization of the ER–Golgi interface for membrane traffic control. *Nature reviews Molecular cell biology* **2013**, *14*, 382.
177. Kirchhausen, T. Bending membranes. *Nature cell biology* **2012**, *14*, 906.
178. Guigas, G.; Weiss, M. Effects of protein crowding on membrane systems. *Biochimica et Biophysica Acta (BBA)-Biomembranes* **2016**, *1858*, 2441–2450.
179. Stachowiak, J.C.; Brodsky, F.M.; Miller, E.A. A cost–benefit analysis of the physical mechanisms of membrane curvature. *Nature cell biology* **2013**, *15*, 1019.
180. Derganc, J.; Copic, A. Membrane bending by protein crowding is affected by protein lateral confinement. *Biochimica et Biophysica Acta (BBA)-Biomembranes* **2016**, *1858*, 1152–1159.
181. Linden, M.; Sens, P.; Phillips, R. Entropic tension in crowded membranes. *PLoS computational biology* **2012**, *8*, e1002431.
182. Van Wylen, G.J.; Sonntag, R.E. Fundamentals of classical thermodynamics. Technical report, 1965.
183. Luding, S. Global equation of state of two-dimensional hard sphere systems. *Physical Review E* **2001**, *63*, 042201.
184. Carnahan, N.F.; Starling, K.E. Equation of state for nonattracting rigid spheres. *The Journal of Chemical Physics* **1969**, *51*, 635–636.
185. Dalbey, R.E. Leader peptidase. *Molecular microbiology* **1991**, *5*, 2855–2860.
186. Kaback, H.R.; Frillingos, S.; Jung, H.; Jung, K.; Prive, G.G.; Ujwal, M.; Weitzman, C.; Wu, J.; Zen, K. The lactose permease meets Frankenstein. *Journal of Experimental Biology* **1994**, *196*, 183–195.
187. Killian, J.A. Hydrophobic mismatch between proteins and lipids in membranes. *Biochimica et Biophysica Acta (BBA)-Reviews on Biomembranes* **1998**, *1376*, 401–416.
188. Thurmond, R.L.; Niemi, A.R.; Lindblom, G.; Wieslander, A.; Rilfors, L. Membrane thickness and molecular ordering in Acholeplasma laidlawii strain A studied by 2H NMR spectroscopy. *Biochemistry* **1994**, *33*, 13178–13188.
189. Andersen, O.S.; Koeppe, R.E. Bilayer thickness and membrane protein function: an energetic perspective. *Annu. Rev. Biophys. Biomol. Struct.* **2007**, *36*, 107–130.
190. Marcelja, S. Lipid-mediated protein interaction in membranes. *Biochimica et Biophysica Acta (BBA)-Biomembranes* **1976**, *455*, 1–7.
191. Owicki, J.C.; McConnell, H.M. Theory of protein-lipid and protein-protein interactions in bilayer membranes. *Proceedings of the National Academy of Sciences* **1979**, *76*, 4750–4754.
192. Lewis, B.A.; Engelman, D.M. Lipid bilayer thickness varies linearly with acyl chain length in fluid phosphatidylcholine vesicles. *Journal of molecular biology* **1983**, *166*, 211–217.
193. Ryba, N.J.; Marsh, D. Protein rotational diffusion and lipid/protein interactions in recombinants of bovine rhodopsin with saturated diacylphosphatidylcholines of different chain lengths studied by conventional and saturation-transfer electron spin resonance. *Biochemistry* **1992**, *31*, 7511–7518.
194. Vonck, J. A three-dimensional difference map of the N intermediate in the bacteriorhodopsin photocycle: part of the F helix tilts in the M to N transition. *Biochemistry* **1996**, *35*, 5870–5878.

195. Rangamani, P.; Benjamini, A.; Agrawal, A.; Smit, B.; Steigmann, D.J.; Oster, G. Small scale membrane mechanics. *Biomechanics and modeling in mechanobiology* **2014**, *13*, 697–711.
196. Duque, D.; Li, X.j.; Katsov, K.; Schick, M. Molecular theory of hydrophobic mismatch between lipids and peptides. *The Journal of chemical physics* **2002**, *116*, 10478–10484.
197. Fattal, D.R.; Ben-Shaul, A. Mean-field calculations of chain packing and conformational statistics in lipid bilayers: comparison with experiments and molecular dynamics studies. *Biophysical journal* **1994**, *67*, 985.
198. Argudo, D.; Bethel, N.P.; Marcoline, F.V.; Wolgemuth, C.W.; Grabe, M. New Continuum Approaches for Determining Protein-Induced Membrane Deformations. *Biophysical journal* **2017**, *112*, 2159–2172.
199. Mouritsen, O.; Bloom, M. Mattress model of lipid-protein interactions in membranes. *Biophysical journal* **1984**, *46*, 141–153.
200. Fournier, J.; Galatola, P. Tubular vesicles and effective fourth-order membrane elastic theories. *EPL (Europhysics Letters)* **1997**, *39*, 225.
201. Siegel, D.P. Fourth-Order Curvature Energy Model for the Stability of Bicontinuous Inverted Cubic Phases in Amphiphile-Water Systems. *Langmuir* **2010**, *26*, 8673–8683.
202. Brannigan, G.; Brown, F.L. Contributions of Gaussian curvature and nonconstant lipid volume to protein deformation of lipid bilayers. *Biophysical journal* **2007**, *92*, 864–876.
203. Kim, K.; Neu, J.; Oster, G. Effect of protein shape on multibody interactions between membrane inclusions. *Physical Review E* **2000**, *61*, 4281.
204. Latorraca, N.R.; Callenberg, K.M.; Boyle, J.P.; Grabe, M. Continuum approaches to understanding ion and peptide interactions with the membrane. *The Journal of membrane biology* **2014**, *247*, 395–408.
205. Israelachvili, J.N. *Intermolecular and surface forces*; Academic press, 2011.
206. Zhou, Y.; Lu, B.; Gorfe, A.A. Continuum electromechanical modeling of protein-membrane interactions. *Physical Review E* **2010**, *82*, 041923.
207. Steigmann, D.; Agrawal, A. Electromechanics of polarized lipid bilayers. *Mathematics and Mechanics of Complex Systems* **2016**, *4*, 31–54.
208. Steigmann, D.J. *The Role of Mechanics in the Study of Lipid Bilayers*; Vol. 577, Springer, 2017.
209. Monzel, C.; Sengupta, K. Measuring shape fluctuations in biological membranes. *Journal of Physics D: Applied Physics* **2016**, *49*, 243002.
210. Shlomovitz, R.; Gov, N.; Roux, A. Membrane-mediated interactions and the dynamics of dynamin oligomers on membrane tubes. *New Journal of Physics* **2011**, *13*, 065008.
211. Peng, Z.; Asaro, R.J.; Zhu, Q. Multiscale simulation of erythrocyte membranes. *Physical Review E* **2010**, *81*, 031904.
212. Noguchi, H.; Gompper, G. Fluid vesicles with viscous membranes in shear flow. *Physical review letters* **2004**, *93*, 258102.
213. Kirchhausen, T.; Owen, D.; Harrison, S.C. Molecular structure, function, and dynamics of clathrin-mediated membrane traffic. *Cold Spring Harbor perspectives in biology* **2014**, *6*, a016725.
214. Ford, M.G.; Mills, I.G.; Peter, B.J.; Vallis, Y.; Praefcke, G.J.; Evans, P.R.; McMahon, H.T. Curvature of clathrin-coated pits driven by epsin. *Nature* **2002**, *419*, 361.
215. Calizo, R.C.; Ron, A.; Hu, M.; Bhattacharya, S.; Janssen, W.G.; Hone, J.; Scarlata, S.; Rangamani, P.; Iyengar, R. Curvature regulates subcellular organelle location to control intracellular signal propagation. *bioRxiv* **2017**, p. 161950.
216. Prevost, C.; Zhao, H.; Manzi, J.; Lemichez, E.; Lappalainen, P.; Callan-Jones, A.; Bassereau, P. IRSp53 senses negative membrane curvature and phase separates along membrane tubules. *Nature communications* **2015**, *6*, 8529.
217. Wedlich-Soldner, R.; Betz, T. Self-organization: the fundament of cell biology, 2018.
218. Ramaswamy, S.; Toner, J.; Prost, J. Nonequilibrium fluctuations, traveling waves, and instabilities in active membranes. *Physical review letters* **2000**, *84*, 3494.
219. Madsen, K.L.; Bhatia, V.; Gether, U.; Stamou, D. BAR domains, amphipathic helices and membrane-anchored proteins use the same mechanism to sense membrane curvature. *FEBS letters* **2010**, *584*, 1848–1855.
220. Raucher, D.; Stauffer, T.; Chen, W.; Shen, K.; Guo, S.; York, J.D.; Sheetz, M.P.; Meyer, T. Phosphatidylinositol 4,5-bisphosphate functions as a second messenger that regulates cytoskeleton-plasma membrane adhesion. *Cell* **2000**, *100*, 221–228.
221. Ayton, G.S.; McWhirter, J.L.; Voth, G.A. A second generation mesoscopic lipid bilayer model: Connections to field-theory descriptions of membranes and nonlocal hydrodynamics. *The Journal of chemical physics* **2006**, *124*, 064906.